Gulf of Trieste, Italy

Application of a normalization procedure in determining regional geochemical baselines

S. Covelli · G. Fontolan

Abstract The regional variability of some geochemical parameters in the Gulf of Trieste is considered in terms of their relationship with Al, used as a normalization factor. Baselines calculated from these relationships are used to determine a simple enrichment factor for each element, defined as the ratio between the actual and predicted baseline value. The normalization procedure permits a new non dimensional reference baseline to be obtained that could help to assess the size of possible anomalies and to provide information on the diffusion and dispersion patterns of pollutants inside the monitored area.

Key words Normalization procedure · Geochemical baselines · Trieste, Italy

Introduction

High degrees of urbanization and the concentration of industrial sites in coastal regions inevitably have led to a strong risk of heavy-metal contamination in the neighboring marine environment. Monitoring of the coastal zone has thus become an essential facet in the assessment and control of anthropogenic impacts on coastal ecosystems, particularly in conservation areas. Fine-grained marine sediments act as scavengers for trace elements and often provide an excellent record of man's impact. However, an objective evaluation of the degree of heavy-metal contamination depends on the choice of an appropriate baseline as a reference level.

Received: 24 August 1995 · Accepted: 15 October 1995

S. Covelli · G. Fontolan (✉)
Dipartimento di Scienze Geologiche, Ambientali e Marine,
Universita degli Studi,
Via E. Weiss 2, 34127 Trieste, Italy

Many authors have used the average shale values of Turekian and Wedepohl (1961) or the average crustal abundance data of Taylor (1964) as reference baselines. The best alternative is to compare concentrations between contaminated and mineralogically and texturally comparable, uncontaminated sediments, i.e., estimating preindustrial content of trace elements from the deepest level of cores after having considered that bioturbation has not occurred (Siegel and others 1994; Faganeli and others 1991). Similarly, data reported by Selli and others (1977) or by Paul and Meischner (1976) have been used as baseline levels in studies of contamination in the Adriatic region (Pavoni and others 1987; Guerzoni and others 1984; Donazzolo and others 1981).

The use of these single baseline levels has the disadvantage of not taking into account natural geochemical variability. Thus, for instance, the use of the average shale values in areas where Cr- or Fe-bearing minerals are present and Cr or Fe are naturally enriched (i.e., in the case reported by Prohic and Juracic 1989) could lead to false anomalies being recognized. Similarly, false anomalies may arise because metal values tend to vary with grain-size, higher concentrations being associated with finer-grained sediments. In recognition of the problem, Loring (1990) and Loring and Rantala (1992) recommend the use of scatterplots of element concentration against grain-size or a grain-size proxy as a means of normalizing geochemical data and distinguishing between natural and anthropogenic enrichments.

Many sedimentological (Brambati 1970; Brambati and others 1982; Brambati and Catani 1988; Ogorelec and others 1991) and geochemical (Stefanini 1968, 1970–71; Macchi 1968; Majori and others 1976; Donazzolo and others 1981; Faganeli and others 1991) studies have been carried out in the Gulf of Trieste, but although natural geochemical backgrounds for the northern Adriatic Sea have been recorded, a reference baseline, which takes account of the marked grain-size variability of the sediments is still lacking. Such a baseline could be an important aid to the location of contaminated areas and to the recognition of anthropogenic inputs.

This research is aimed at determining the natural variability in some geochemical parameters in the Gulf of Trieste and defining regional normalization functions that could be useful in the assessment of sediment quality in the area. The procedures could be applied to other similar environments.

Study area

The Gulf of Trieste (Fig. 1) is located in the northeastern Adriatic Sea, with a seaward geographical limit corresponding to the transept Rt. Savudrija-Grado. In general, water depths are shallow, reaching only −25 m in the central part of the Gulf. The main terrigenous sediment supply comes from the Isonzo River, which has a drainage basin of 3430 km^2, extending into both Italy and Slovenia. The drainage area is underlain by two main lithologies: Mesozoic limestone and Eocene flysch. The latter is characterized by an alternating sequence of sandstones and marls in the hilly and prealpine areas bordering the plain, while marls, sandstones, calcarenites, carbonate conglomerates, and breccias prevail in the northernmost alpine chains (Stefanini 1976). The marine area near the river mouth is dominated by carbonate sediments, derived from the Isonzo. Only the southeasternmost sector of the gulf, marked by ephemeral terrigenous inputs from two small rivers, the Rosandra and the Rizana, has significant quantities of quartz–feldspathic material (Brambati 1970).

Textural variation in the sediments of the Gulf of Trieste can be related to the terrigenous input from the Isonzo River, the seabed morphology, and to currents and wave motion.

The delta of the Isonzo extends seaward in a linear fashion, testifying to the prevalence of fluviatile sediment transport over wave dispersion phenomena (Brambati 1970). Sediment dispersion from the Isonzo is symmetrical towards both the northeast and southwest (Brambati and Venzo 1967; Giorgetti and others 1968; Brambati 1970; Brambati and others 1982; Brambati and Catani 1988). Coarse sediments, mainly medium to fine sands and pelitic sands, are dispersed as bed-load by longshore currents both westward to Panzano Bay and eastward to Grado, respectively. There, they mix with residual deposits of similar grain-size belonging to the Mula di Muggia bank and the Quarantia, features which are related to ancient Isonzo deltas (Brambati and others 1982).

Suspended sediment is transported symmetrically from the river mouth as a spreading plume, without significant wave influence. The distribution pattern of fine deposits is therefore related to the decrease of fluviatile influences, and the sediments progressively decrease in grain-size, from very sandy pelites not far from the river mouth, to pelites in the mid-gulf and at depths greater than 6–7 m in Panzano Bay (Brambati and others 1983). Only a small amount of the Isonzo suspended sediment crosses the Rt. Savudrija-Grado boundary, into the marine area far from the northern Adriatic coast (Brambati and Venzo 1967; Brambati 1970; Brambati and Catani 1988). This same boundary separates two areas that are mineralogically different – an illitic area to the east where illite, kaolinite, and chlorite are present, and a montmorillonitic area to the west where montmorillonite, in addition to the other mentioned clay minerals, can be found (Brambati 1968).

The sediment accumulation rate in the central part of the Gulf of Trieste is at about 1 mm yr^{-1} based on ^{210}Pb activity data, but increases to about 2.5 mm yr^{-1} in the direction of the mouth of the Isonzo (Ogorelec and others 1991). Higher values (5.3 mm yr^{-1}) were found in surficial deposits of the inner part of the Koper and Piran bays (Faganeli and others 1991).

Fig. 1
Study area. Points indicate core sampling stations

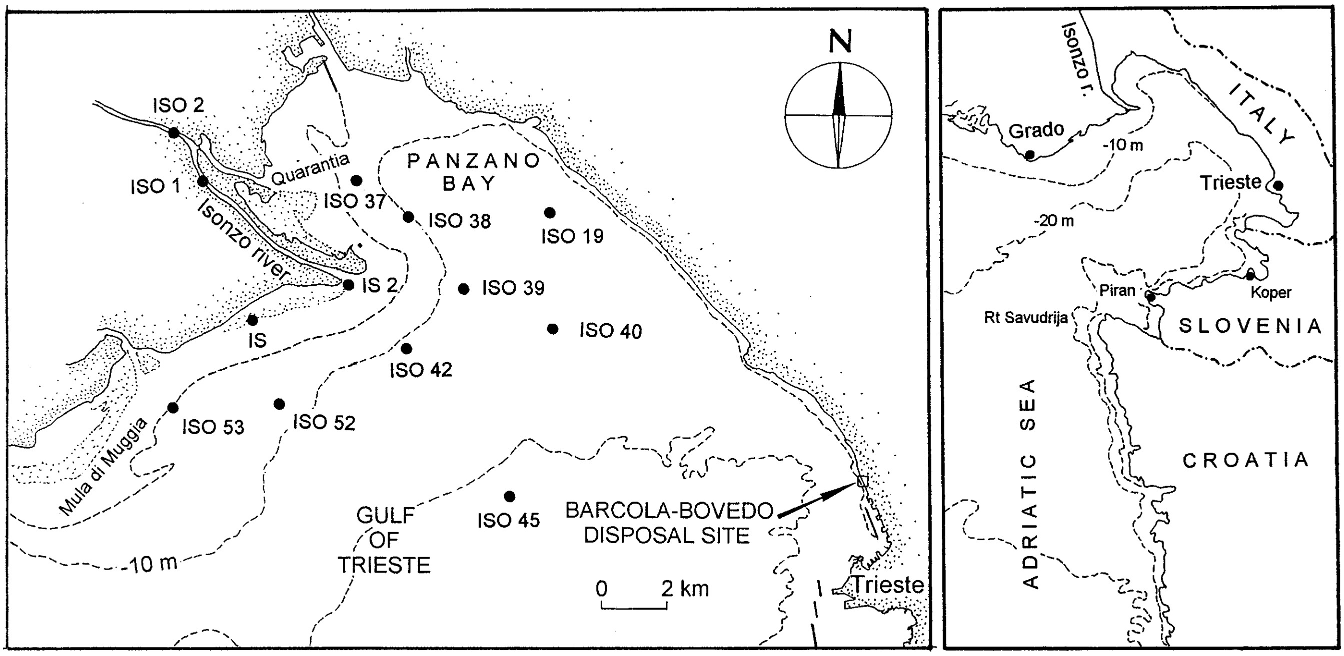

Materials and methods

Thirteen cores, 30–87 cm long, were manually collected on the river banks or by scuba diving using 8-cm-diameter PVC liners (Fig. 1). Each core has been logged and representative samples of 2-cm thickness taken to give a total of 71 samples. All samples were subsampled and subjected to both grain-size and geochemical analysis.

For grain-size analysis, specimens were heated in a water bath for 48 h with 10 vol H_2O_2, then treated ultrasonically for 5 min and finally wet-sieved with a 53-μm sieve. The sandy fraction ($53 < \text{diam} < 2000$ μm) was washed, dried, and then analyzed by sieve (1/2 ϕ Dutch-scale). The pelitic fraction ($\text{diam} < 53$ μm) was resuspended in distilled water, centrifuged, treated with 0.5 g dm^{-3} Na hexametaphosphate antiflocculant solution, and then analyzed using a Micromeritics Sedigraph 5000 ET Particle Size Analyser. The textural composition of the samples was defined using the bivariate (sand–pelite proportion) nomenclature of Nota (1958), 2 μm was used as the boundary between silt and clay.

Several analytical procedures for the determination of heavy metals in marine sediments are described in the literature. In this study, a total decomposition method using HF + aqua regia before AAS analyses, as recommended by Loring and Rantala (1992), was used on the <2-mm sediment fraction to yield the total metal concentration in the whole sediment. This is in accordance with the criteria on which international dredging and dumping regulations are based. The use of chemical data from unfractionated samples means that the technique is applicable to a wide range of sediment types, minimizing difficulties in the selection of baseline or reference concentrations, and avoiding time-consuming separation of the finest fractions (Rule 1986).

Subsamples for geochemical analysis were dried at 40 °C, and granules and organic debris were removed by sieving. The sample was then ground to pass a 200-mesh (75-μm) sieve and dried overnight at 110 °C. Samples were then treated with a mixture of HF, HNO_3, and $HClO_4$ acids following the procedure proposed by Bruland and others (1974).

The concentrations of Cu, Cr, Ni, Pb, Zn, Li, and Al were determined using a Perkin Elmer 5000 AAS. Fe was determined by the phenanthroline method and P by the stannous chloride method, both using a double-ray Perkin Elmer model 124 (Visible) Spectrophotometer, following the Standard Methods for the Examination of Water and Wastewater (SMEWW) (Rand and others 1976). Organic carbon was determined using a modified Walkley-Black titration method reported by Gaudette and others (1974). C, H, and N analyses were carried out using a Perkin-Elmer 2400 CHN Elemental Analyser. Ca and Mg contents were determined by titration using and EDTA-Na_2 solution following the SMEWW (Rand and others 1976). The Systat PC statistical package was used for graphical and numerical manipulations.

Results

Grain-size and geochemical data are reported in Tab. 1. Grain-size variations in the cores are related to the different dispersion patterns of sediment from the Isonzo and to the alternation of layers representing different fluviatile regimes. In general, pelites (77.10% ± 26.14) dominate over sands (22.90% ± 26.14). The finest component is mainly silt (47.70% ± 14.69) followed by clay (29.40% ± 15.36). Sandy sediments are more common in cores collected in the river banks and in the inner delta, whereas pelitic material prevails in the whole outer delta and in the mid-gulf.

Variable thicknesses of deltaic deposits are superimposed on residual coarser ones in some distal cores (ISO 45, 40, and 52) and are marked by a noticeable decrease in pelite content towards the bottom. Organic carbon (C_{org}) concentrations average 0.81% ± 0.36 and total C (C_{tot}) contents, 6.57% ± 1.38. Average H and N values are 0.41% ± 0.17 and 0.08% ± 0.03, respectively, while total P (P_{tot}) varies between 120 and 505 ppm (average: 338 ppm ± 101).

Among the major elements, Ca (average 14.99% ± 3.64) contents are higher than Al (3.97% ± 1.57), Mg (3.53% ± 0.84), and Fe (2.24% ± 0.89), while among the trace metals, Ni has the highest average concentration (110 ppm ± 31), followed by Pb (91 ppm ± 26), Cr (77 ppm ± 30), Zn (72 ppm ± 29), Li (38 ppm ± 15), and Cu (28 ppm ± 12).

Ca and Mg show a progressive decrease in concentration from the inner delta area to the mid-gulf, with maximum concentrations in Banco del Becco (west branch of the Isonzo delta) where the highest organic C contents were also observed. Al, Fe, Li, Cr, Zn, and, to a lesser extent, Ni show a contrasting trend, progressively increasing in level seaward. Cu follows a similar trend, but with a concentration decrease in the most distal area investigated.

Normalization procedure

Previous work

Many authors have pointed out that in marine sediments there is a good positive correlation between trace metal concentration and the proportion of fine-grained material, although the definition of what constitutes "fine-grained" varies (de Groot and others 1976; Donazzolo and others 1981; De Rosa and others 1981; Brambati and Marocco 1984; Loring and Nota 1973; Loring 1978; Loring and Rantala 1992). To compensate for grain-size and mineralogy effects on trace element concentrations and to assess if anomalous metal contributions are present, a common approach is to normalize the geochemical data using one element as a grain-size proxy. The normalizing element must be an important constituent of one or more of the major trace metal carriers and reflect their granular variability in the sediments (Loring 1990). The choice of grain-size proxy is not universal but depends,

Tab. 1
Grain-size and geochemical data

Core	Label	Level (cm)	Sand (%)	Silt (%)	Clay (%)	C_{tot} (%)	C_{org} (%)	H (%)	N (%)	P_{tot} (ppm)	Ca (%)	Mg (%)	Al (%)	Fe (%)	Li (ppm)	Cr (ppm)	Ni (ppm)	Cu (ppm)	Zn (ppm)	Pb (ppm)
IS	A	0– 3	42.89	44.71	12.40	7.83	1.30	0.33	0.11	238	17.11	3.83	1.98	1.19	20	48	48	16	60	92
IS	B	15–17	31.94	54.31	13.75	8.03	1.50	0.38	0.14	344	15.33	4.18	2.53	1.45	24	52	44	20	80	92
IS	C	28–30	42.99	41.17	15.84	7.92	1.34	0.31	0.11	301	16.31	4.27	2.29	1.31	20	44	44	20	60	84
IS 2	A	0– 2	37.51	39.25	23.24	7.71	0.82	0.34	0.09	315	17.27	3.78	3.11	1.79	28	56	60	32	72	136
IS 2	B	14–16	75.49	16.05	8.46	9.59	0.31	0.12	0.03	203	24.50	4.50	1.43	0.77	16	24	36	16	56	76
IS 2	C	32–34	39.54	49.66	10.80	7.56	0.34	0.14	0.02	222	17.61	4.71	2.24	1.26	20	40	44	16	44	76
IS 2	D	48–50	1.14	67.72	31.14	3.70	1.14	0.53	0.10	350	8.38	1.99	6.06	3.50	56	124	120	44	88	88
IS 2	E	56–58	44.57	34.82	20.61	7.13	0.52	0.25	0.04	234	17.65	3.78	3.38	1.75	28	60	60	24	52	56
IS 2	F	64–66	51.00	35.03	13.97	7.91	0.58	0.23	0.04	224	19.76	4.07	2.63	1.46	24	48	60	24	52	76
ISO 1	A	2– 4	29.59	50.70	19.71	7.85	0.79	0.34	0.08	336	17.30	4.35	2.93	1.70	24	56	48	24	84	95
ISO 1	B	6– 8	48.66	43.00	8.34	8.13	0.50	0.20	0.04	232	18.10	4.84	1.87	1.21	20	40	111	20	48	56
ISO 1	C	10–12	24.09	61.41	14.50	6.69	0.91	0.30	0.06	258	14.10	4.03	3.51	1.97	32	64	100	20	40	64
ISO 1	D	14–16	50.36	39.31	10.33	8.28	0.82	0.22	0.04	204	18.94	4.37	2.08	1.41	20	44	108	16	36	56
ISO 1	E	27–29	56.61	37.44	5.95	8.18	0.67	0.17	0.03	191	18.57	4.93	1.80	1.28	16	40	119	16	32	52
ISO 1	F	43–45	81.62	14.83	3.55	9.23	0.23	0.07	0.00	132	20.79	4.85	1.11	0.47	12	20	114	8	8	44
ISO 1	G	50–52	73.26	21.47	5.27	7.34	0.45	0.13	0.03	149	15.73	5.33	1.52	0.71	16	32	100	8	12	52
ISO 1	H	59–61	76.11	21.29	2.60	7.55	0.37	0.11	0.02	120	15.68	5.47	1.34	0.58	16	24	96	8	34	88
ISO 1	I	67–69	72.69	21.71	5.60	7.81	0.44	0.12	0.03	143	17.92	5.05	1.41	0.67	16	36	112	12	8	48
ISO 1	L	71–73	86.87	11.20	1.93	9.29	0.17	0.06	0.01	137	22.52	5.06	0.89	0.43	8	24	104	4	12	66
ISO 1	M	83–85	83.28	13.17	3.55	8.79	0.24	0.07	0.03	140	21.04	4.79	1.07	0.46	12	24	95	8	12	64
ISO 2	A	1– 3	46.69	37.16	16.15	8.18	0.75	0.29	0.08	336	19.27	4.25	2.23	1.40	20	40	119	16	60	91
ISO 2	B	11–13	45.96	38.29	15.75	8.30	0.46	0.25	0.07	275	19.62	4.03	2.28	1.36	20	40	100	20	60	92
ISO 2	C	16–18	13.78	58.63	27.59	6.34	0.78	0.42	0.10	383	13.96	3.53	4.07	2.35	32	64	147	24	68	92
ISO 2	D	20–22	72.08	20.10	7.82	9.50	0.35	0.16	0.04	193	25.12	3.73	1.42	0.83	12	24	143	8	40	88
ISO 2	E	30–32	31.00	51.66	17.34	7.18	0.60	0.32	0.06	307	16.62	4.05	3.19	1.87	24	56	139	20	60	107
ISO 2	F	34–36	10.16	57.95	31.89	5.87	2.06	0.62	0.12	412	8.95	3.78	5.05	3.19	56	92	104	28	72	52
ISO 2	G	47–49	4.08	74.71	21.21	7.18	2.32	0.58	0.11	358	9.75	4.75	4.19	2.51	44	76	116	28	60	52
ISO 19	A	2– 4	0.96	45.56	53.48	5.08	1.17	0.71	0.15	426	10.41	2.38	5.83	3.38	60	112	148	44	128	158
ISO 19	B	16–18	1.92	46.10	51.98	4.71	0.80	0.64	0.10	421	10.95	2.57	6.02	3.44	60	104	152	36	96	151
ISO 19	C	32–34	1.48	47.73	50.79	4.62	0.70	0.60	0.07	342	11.36	2.52	5.98	3.42	60	108	132	32	100	81
ISO 37	A	4– 6	24.92	44.90	30.18	6.99	0.87	0.49	0.10	391	16.65	3.44	3.77	2.10	36	80	108	36	88	120
ISO 37	B	11–13	47.19	35.91	16.90	8.33	0.59	0.27	0.06	265	20.53	4.10	2.31	1.48	24	60	119	32	64	91
ISO 37	C	20–22	27.75	43.35	28.90	7.19	0.70	0.38	0.04	337	17.41	3.48	3.42	2.00	32	80	116	24	84	108
ISO 37	D	38–40	0.68	59.10	40.22	6.45	0.89	0.46	0.07	422	15.07	3.44	4.50	2.50	40	84	115	28	64	88
ISO 37	E	59–61	2.52	54.59	42.89	5.45	0.75	0.53	0.07	433	13.17	2.86	5.07	3.00	48	108	135	36	48	104
ISO 38	A	2– 4	0.67	58.60	40.73	6.15	1.03	0.60	0.12	450	13.34	3.15	4.96	2.86	48	92	128	36	108	124
ISO 38	B	6– 8	0.93	59.64	39.43	6.16	0.99	0.57	0.10	441	13.49	3.29	5.03	2.82	44	92	163	36	104	112
ISO 38	C	9–11	0.61	55.66	43.73	6.04	0.92	0.56	0.09	433	13.40	3.29	4.98	2.88	44	92	99	40	107	119
ISO 38	D	22–24	0.62	58.63	40.75	5.82	0.69	0.46	0.08	414	13.70	3.06	5.05	2.86	48	96	72	36	68	108
ISO 38	E	41–43	0.13	54.43	45.44	4.55	0.72	0.58	0.09	450	10.30	2.76	5.89	3.37	56	112	104	40	104	60
ISO 39	A	2–4	0.34	51.34	48.32	5.82	0.99	0.63	0.13	481	12.40	2.87	5.28	3.03	50	101	159	54	128	144
ISO 39	B	10–12	0.49	53.74	45.77	5.66	0.94	0.58	0.11	458	13.08	2.86	5.30	3.03	48	107	88	36	131	123
ISO 39	C	14–16	1.13	53.88	44.99	5.69	0.82	0.57	0.12	505	13.36	2.91	5.32	2.95	48	100	92	36	112	116
IOS 39	D	22–24	0.42	51.78	47.80	5.59	0.78	0.55	0.09	436	13.43	2.86	5.24	3.06	52	108	96	36	104	120
ISO 39	E	40–42	0.46	53.75	45.79	4.54	0.66	0.59	0.07	359	10.57	2.67	5.83	3.33	56	116	100	36	86	120
ISO 39	F	62–64	1.03	46.52	52.45	4.02	0.65	0.63	0.09	356	9.53	2.43	6.53	3.59	64	124	102	32	90	104
ISO 40	A	4– 6	3.46	45.12	51.42	5.03	0.96	0.61	0.13	461	12.02	2.43	5.55	3.17	57	113	128	57	140	131
ISO 40	B	18–20	5.70	43.01	51.29	4.71	0.61	0.58	0.08	393	12.25	2.19	5.85	3.30	60	112	100	32	68	60
ISO 40	C	43–45	10.84	44.58	44.58	5.53	0.58	0.46	0.10	279	14.72	2.57	5.09	2.65	52	96	86	20	60	72
ISO 40	D	60–62	30.84	32.32	36.84	6.71	0.49	0.38	0.04	254	18.73	2.43	3.79	2.19	40	74	64	20	48	96
ISO 42	A	0– 2	1.32	60.19	38.49	6.51	1.01	0.54	0.11	457	14.02	3.53	4.67	2.63	40	95	127	36	87	99
ISO 42	B	15–17	0.76	59.54	39.70	6.37	0.99	0.49	0.09	418	14.46	3.35	4.82	2.70	40	92	159	32	96	84
ISO 42	C	34–36	0.87	56.50	42.63	6.16	0.74	0.47	0.07	436	14.64	3.28	5.01	2.79	44	91	123	36	79	99
ISO 42	D	55–57	0.16	56.41	43.43	4.74	0.66	0.52	0.07	430	11.28	2.67	5.90	3.20	52	108	156	48	64	60
ISO 45	A	4– 6	10.22	39.25	50.53	5.35	0.88	0.59	0.12	387	12.50	2.63	5.38	2.90	52	108	144	32	98	104
ISO 45	B	25–27	21.11	37.87	41.02	5.73	0.47	0.48	0.06	306	15.82	2.72	4.62	2.46	48	92	163	20	72	80
ISO 45	C	49–51	33.00	31.00	36.00	6.55	0.38	0.37	0.04	246	18.42	2.62	3.62	2.06	40	80	148	16	72	116
ISO 52	A	2– 4	1.51	65.99	32.50	6.75	1.05	0.50	0.11	443	14.37	3.68	4.40	2.40	40	88	115	36	96	80
ISO 52	B	11–13	1.04	66.64	32.32	6.83	1.02	0.48	0.10	417	14.81	3.79	3.98	2.35	36	88	132	36	104	84

Table 1 Continued

Core	Label	Level (cm)	Sand (%)	Silt (%)	Clay (%)	C_{tot} (%)	C_{org} (%)	H (%)	N (%)	P_{tot} (ppm)	Ca (%)	Mg (%)	Al (%)	Fe (%)	Li (ppm)	Cr (ppm)	Ni (ppm)	Cu (ppm)	Zn (ppm)	Pb (ppm)
ISO 52	C	15–17	1.44	70.68	27.88	6.91	0.90	0.43	0.09	418	15.13	3.84	4.73	2.12	36	80	124	44	104	100
ISO 52	D	31–33	3.35	62.34	34.31	6.44	1.02	0.48	0.09	406	14.69	3.28	4.74	2.60	40	91	115	32	99	119
ISO 52	E	38–40	2.69	60.33	36.98	5.11	0.89	0.52	0.07	409	11.53	2.91	5.83	3.06	52	104	116	36	68	128
ISO 52	F	58–60	7.12	55.73	37.15	5.09	0.98	0.54	0.08	403	11.22	2.63	5.79	3.13	56	100	120	32	80	72
ISO 52	G	82–84	23.43	49.64	26.93	6.53	0.73	0.37	0.05	328	16.19	3.16	3.82	2.26	40	80	116	24	68	80
ISO 53	A	4– 6	51.36	38.76	9.88	7.80	0.36	0.21	0.02	224	17.80	4.60	1.96	1.26	20	44	116	12	48	76
ISO 53	B	12–14	9.61	66.77	23.62	6.60	1.04	0.43	0.08	350	13.67	3.78	3.69	2.18	36	82	124	28	60	80
ISO 53	C	34–36	10.28	68.88	20.84	6.07	0.91	0.38	0.07	348	12.63	3.64	3.88	2.24	36	76	88	28	64	80
ISO 53	D	54–56	1.93	64.24	33.83	5.52	1.00	0.49	0.09	401	11.45	3.06	4.84	2.82	44	100	108	32	72	76
ISO 53	E	74–76	3.82	58.67	37.51	5.34	0.98	0.51	0.12	413	11.21	3.06	5.16	2.90	48	104	140	36	80	80
ISO 53	F	79–81	1.43	56.96	41.61	4.61	1.12	0.63	0.10	445	8.97	2.53	6.00	3.34	56	128	140	52	96	112
ISO 53	G	85–87	0.74	63.03	36.23	5.64	1.07	0.51	0.14	399	11.85	3.11	4.81	2.66	44	96	120	52	78	76
Average			22.90	47.70	29.40	6.57	0.81	0.41	0.08	338	14.99	3.53	3.97	2.24	38	77	110	28	72	91
SD			26.14	14.69	15.36	1.38	0.36	0.17	0.03	101	3.64	0.84	1.57	0.89	15	30	31	12	29	26
Min			0.13	11.20	1.93	3.70	0.17	0.06	0.00	120	8.38	1.99	0.89	0.43	8	20	36	4	8	44
Max			86.87	74.71	53.48	9.59	2.32	0.71	0.15	505	25.12	5.47	6.53	3.59	64	128	163	57	140	158

among other things, on the study area and the anthropogenic wastes which are involved.

Al, which is one of the most important constituents of the aluminosilicate mineral fraction, is often used as a grain-size proxy (Windom and others 1989; Bruland and others 1974; Hirst 1962; Helz and others 1983; Din 1992). However, Loring (1990) has shown that Li is superior to Al for the normalization of metal data from sediments derived mainly from the glacial erosion of crystalline rocks and is equal or superior to Al for those derived from noncrystalline rocks. It is possible to use Fe as normalizing element when its anthropogenic inputs are lower than the natural ones (Trefry and Presley 1976; Sinex and Wright 1988; Rule 1986). Ackermann (1980) chose Cs after a comparison of several potential normalizing elements (Cs, Eu, Fe, Rb, Sc, Sm, and Th).

Whenever a possible anthropogenic input of a grain-size proxy is suspected, a preliminary investigation of contaminant types is recommended before choosing the reference element. The Humber Estuary (UK) receives effluents from an industrialized zone, including titanium dioxide processing factories, and shows high levels of Fe, Ti, V, Ni, Y, and Al. For this reason Grant and Middleton (1990) and Ciavola and Covelli (1994) normalized to Rb, which is not anthropogenically enriched. An evaluation of the correlation between possible grain proxies and metals, using a correlation matrix or scatterplots, is recommended as an aid to making the correct choice.

The value of eliminating the grain-size effect on metal data is illustrated by Allen and Rae (1987) in a study of the Severn Estuary (UK), in which they develop a chemostratigraphy for recent deposits affected by both natural and anthropogenic inputs. Using a technique based on normalization of metal values to Rb, chosen as proxy for grain-size, the authors calculate nondimensional metal index (l_m) values for sediment samples from the linear formula:

$$l_m = (C_m - y_m)/C_{Rb}$$

where C_m is the measured metal concentration in the sample, y_m the concentration in the estuarine sediments at zero Rb content, and C_{Rb} the measured Rb concentration. Vertical variability of l_m reveals a temporal pattern that allows the sedimentary record to be characterized in terms of chemozones. It does not, however, quantify the anthropogenic inputs.

For the estimation of anthropogenic inputs, it is more useful to calculate the degree of enrichment of an element by dividing its ratio to the normalizing element by the same ratio found in the chosen baseline (Middleton and Grant 1990) to yield a nondimensional enrichment factor (*EF*):

$$EF = (X/Y)_{sample}/(X/Y)_{baseline}$$

where X is the concentration of the potentially enriched element and Y is the concentration of the proxy element. A value of unity denotes no enrichment or depletion relative to the baseline. This general method has been used in many works (Ciavola and Covelli 1994; Grant and Middleton 1990; Rule 1986; Sinex and Helz 1981), although based on different normalizing elements and methods of baseline determination.

Sinex and Helz (1981) reported that *EF*s are generally not very sensitive to the choice of a baseline. They compared normalizing data to Turekian and Wedepohl's (1961) average shale and Taylor's (1964) average crust values, and showed that *EF*s for most elements would change by less than 10%. Exceptions were Zn, Cd, and Pb for which the *EF* would decrease by 40–50% using average crust baseline values. Siegel and others (1994) ignored the grain-size proxy factor and used the cultural enrichment factor (*CEF*) proposed by Ferguson (1990). This is simply the ratio between the mean metal concentration in the <2-μm fraction of a 20-cm thickness of superficial sediment and the corresponding concentration in the baseline. Preindustrial baseline data are obtained from deepest levels of cores, assumed to be uncontaminated on the basis of estimates of the sedimentation rate and vertical concentration profiles.

Muller (1969) assessed the degree of metal pollution by means of seven different classes based on the numerical values of the index of geoaccumulation (I_{geo}):

$$I_{geo} = \log_2 C_n / 1.5\ B_n$$

where C_n is the measured concentration of element n in the sediment or size fraction, and B_n is the background concentration of the element n, either directly measured in texturally equivalent uncontaminated sediments or size fractions or taken from the literature. The factor 1.5 is introduced to include possible differences in the background values due to lithological variations.

From this brief review it is clear that there is no uniform approach to the determination of baseline geochemical reference levels and the quantification of anthropogenic inputs and, moreover, that the use of standard shale or crust values or simple normalization ratios does not solve the more complex situations, as in cases involving great grain-size variability.

Loring (1990) and Loring and Rantala (1992) emphasize the importance of regional variability scatterplots of geochemical parameters against normalizing elements or grain-size as a means of identifying anomalous values. It would clearly be helpful to have a mathematical expression of these functions to simplify the comparison among samples, determine the degree of enrichment for individual elements, and to help identify areas which have been affected by anthropogenic contamination.

Data processing

By means of a data correlation matrix (Tab. 2), the relationship between the clay content, possible grain-size proxy elements, and trace elements can be examined. Graphs illustrating the relationships are shown in Fig. 2. There is good correlation between all the potential grain-size proxies and the clay content, shown by the very high values of Pearson's correlation coefficient (clay vs Al: $r = 0.944$; clay vs Fe: $r = 0.938$; clay vs Li: $r = 0.942$; with $P < 0.001$). On the whole, Al seems to be the best grain-size proxy and is used in the following normalization procedures.

The linear relationships between each metal and Al were determined, in the form of $y = ax + b$ (Tab. 3), where y is the predicted metal value and x is the Al concentration in the sample. As proposed by Loring and Rantala (1992), the 95% confidence band was estimated by means of the Systat Smooth Procedure, thus defining a range of data variability around each significant ($P < 0.001$) regression line. On the basis of the above equation, a predicted value for each element and sample was computed from the Al content. The ratios between real and predicted values then were obtained, and the standard deviation (σ) calculated. In such a manner, a regional reference (background) range for each element was obtained as $1 \pm 2\sigma$. The ratio between real and predicted values can be defined as an enrichment factor (*EF*). The cumulative frequency graphs shown in Fig. 3 illustrate the narrow background range of the *EF* values, which has a maximum of 1 ± 0.5. The range width decreases when the correlation coefficient with Al increases and is reflected in the slope of the cumulative curve. Results lying outside the range $1 \pm 2\sigma$ can be classed as potentially anomalous and are easily discernible on the graphs. Departures from linearity in the cumulative frequency graph may also indicate anomalous data.

Table 2
Correlation matrix of grain-size and geochemical data

	Sand	Silt	Clay	C_{tot}	C_{org}	H	N	P_{tot}	Ca	Mg	Al	Fe	Li	Cr	Ni	Cu	Zn	Pb
Sand	1.000																	
Silt	−0.864	1.000																
Clay	−0.876	0.513	1.000															
C_{tot}	0.845	−0.590	−0.873	1.000														
C_{org}	−0.548	0.681	0.282	−0.312	1.000													
H	−0.936	0.697	0.927	−0.863	0.583	1.000												
N	−0.733	0.642	0.634	−0.548	0.740	0.798	1.000											
P_{tot}	−0.928	0.779	0.834	−0.716	0.549	0.906	0.794	1.000										
Ca	0.836	−0.727	−0.726	0.906	−0.605	−0.852	−0.666	−0.729	1.000									
Mg	0.778	−0.436	−0.908	0.848	−0.190	−0.828	−0.545	−0.702	0.627	1.000								
Al	−0.934	0.674	0.944	−0.947	0.407	0.948	0.650	0.854	−0.863	−0.886	1.000							
Fe	−0.939	0.690	0.938	−0.938	0.450	0.959	0.664	0.863	−0.867	−0.881	0.990	1.000						
Li	−0.884	0.589	0.942	−0.948	0.405	0.940	0.623	0.790	−0.860	−0.890	0.978	0.977	1.000					
Cr	−0.923	0.661	0.938	−0.944	0.404	0.942	0.647	0.842	−0.852	−0.893	0.978	0.977	0.968	1.000				
Ni	−0.356	0.218	0.398	−0.377	0.052	0.401	0.179	0.354	−0.322	−0.344	0.397	0.397	0.380	0.406	1.000			
Cu	−0.840	0.676	0.783	−0.740	0.450	0.836	0.722	0.867	−0.726	−0.704	0.830	0.827	0.779	0.840	0.349	1.000		
Zn	−0.793	0.586	0.790	−0.627	0.441	0.837	0.773	0.853	−0.594	−0.688	0.757	0.764	0.719	0.758	0.278	0.811	1.000	
Pb	−0.454	0.225	0.557	−0.361	0.121	0.533	0.486	0.543	−0.265	−0.515	0.454	0.455	0.424	0.455	0.193	0.519	0.690	1.000

$r > 0.370$ corresponds to $P < 0.001$

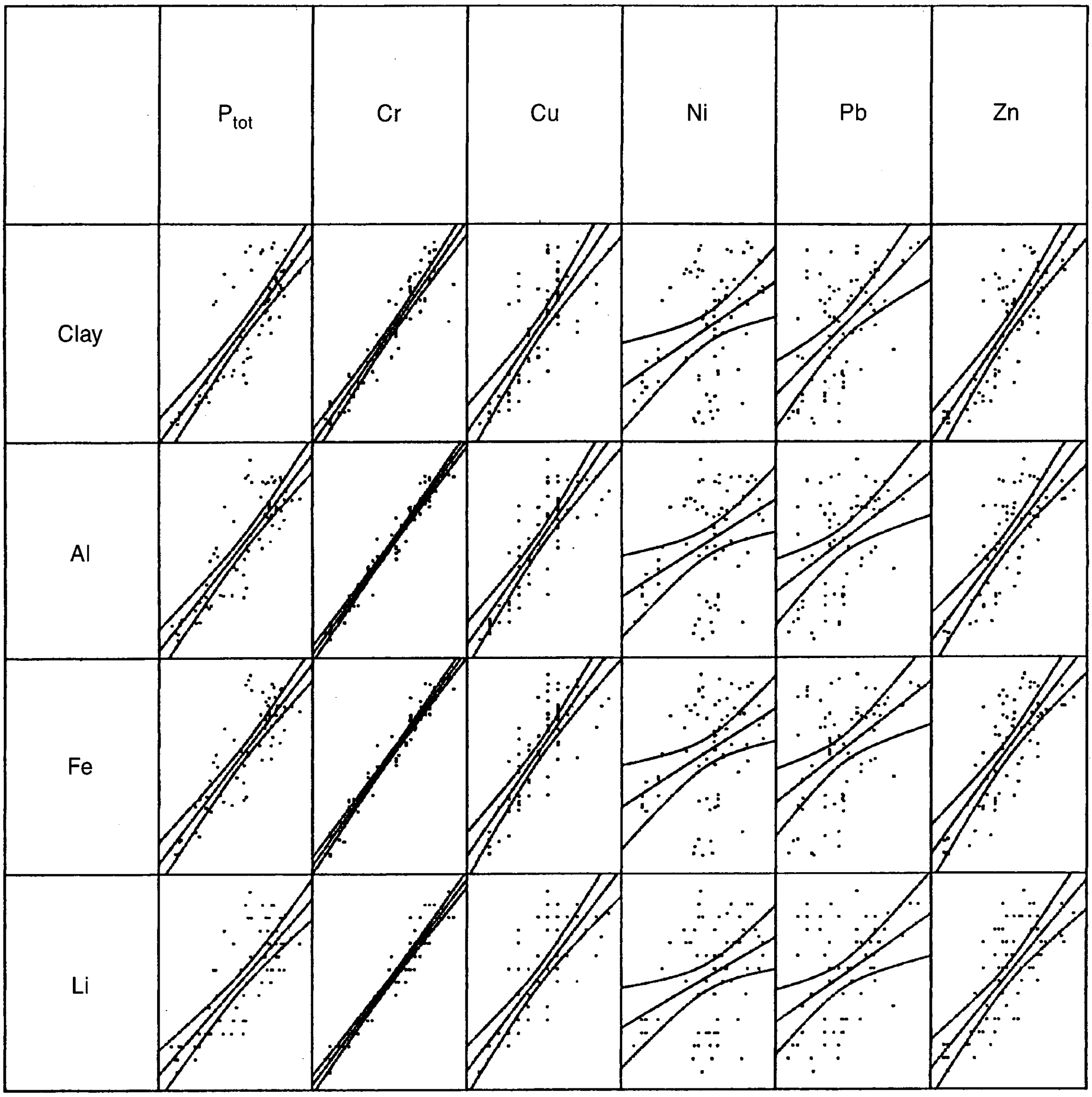

Fig. 2
Scatterplot matrix between clay content, grain-proxy elements and trace elements. The regression line and 95% confidence band are reported as computed by Systat smooth procedure

Table 3
Linear relationship between metals and Al

Equation	SEE	*r, P*
Fe = 0.558 Al + 0.030	0.129	0.990, <0.001
Li = 9.400 Al + 0.190	3.180	0.978, <0.001
Cr = 18.482 Al + 3.955	6.297	0.978, <0.001
Cu = 6.285 Al + 3.431	6.733	0.830, <0.001
Ni = 7.804 Al + 78.753	28.800	0.397, <0.001
Zn = 14.091 Al + 16.244	19.435	0.757, <0.001
Pb = 7.484 Al + 60.853	23.416	0.454, <0.001

[1] SEE indicates the standard error of *Y* extimation, whereas *r* and *P* refer to Tab. 2

Discussion

The areal, as well as the vertical, grain-size variability of the cores reflects the strong influence of the Isonzo River sediment on most of the Gulf of Trieste. As previously pointed out, all samples collected along the river (ISO 1, ISO 2) and cores located in the inner delta (IS 2, IS, ISO 37, ISO 53) (Fig. 1) have a significant sand content, mainly in the more surficial layers, which may be used as markers of the nearshore dispersion of coarse material. Wave-dispersion phenomena are very limited, and the Isonzo delta can be defined as a river-dominated type. The outer delta is mainly characterized by pelites spreading radially from the river mouth (Brambati 1970; Brambati and Catani 1988), and the external limit is defined by the outcropping of coarser residual material (ISO 45), belonging to littoral sediments deposited during the Flandrian transgression (Van Straaten 1965; Brambati and

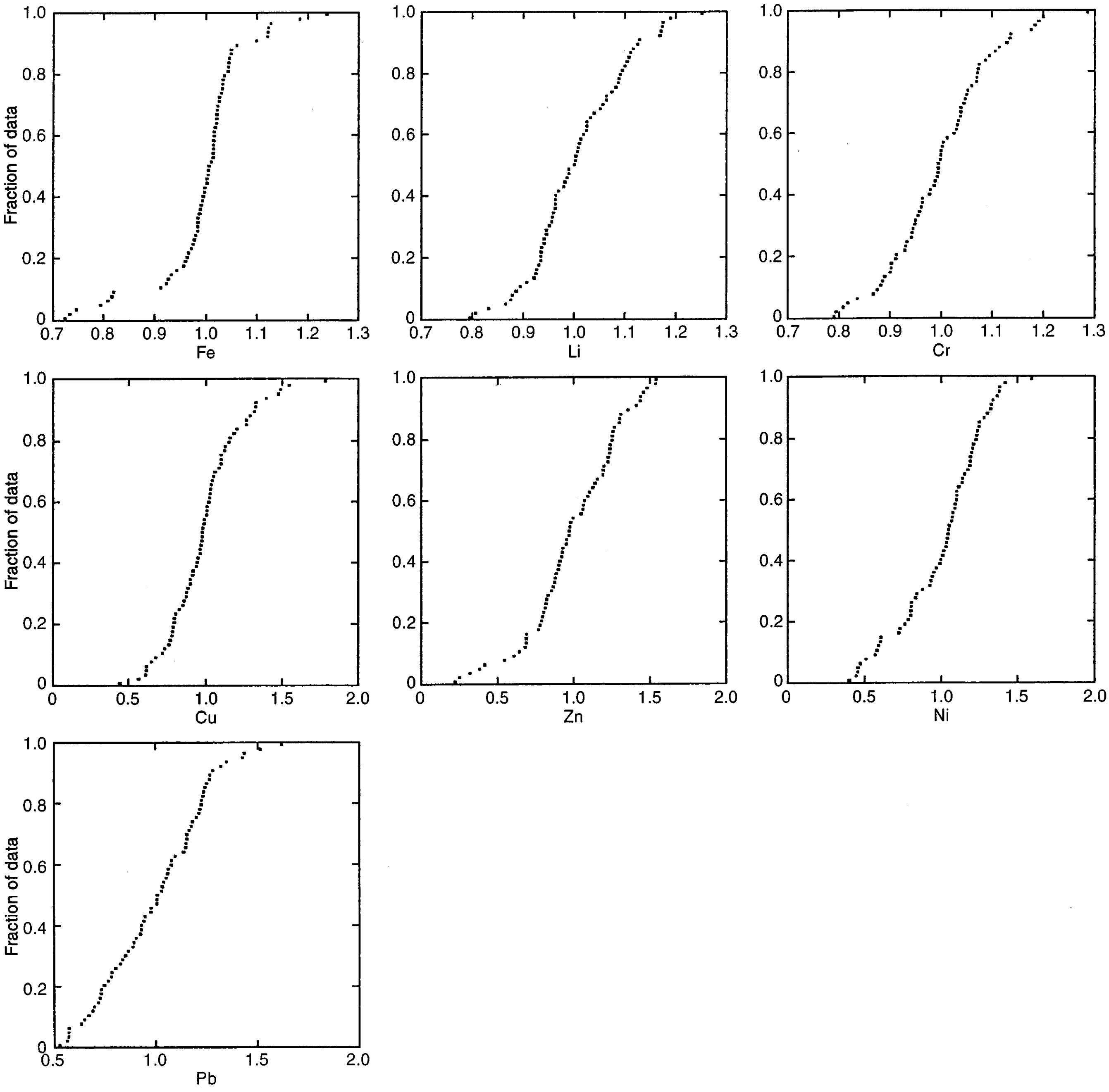

Fig. 3
Cumulative fraction of *EF* data

Venzo 1967). The record of this transgression is also present in coarser, basal deposits, overlapped by finer, essentially pelitic material in cores ISO 40 and ISO 52.

In the geochemical data, the high values of Ca indicate the contribution of detrital carbonate to the gulf deposits, which belong to the Calcitic Subprovince (Brambati 1970). Mg and C_{tot} may also be related to the carbonate contribution as suggested by Mg–Ca and C_{tot}–Ca correlation coefficients of $r = 0.63$ and 0.91 ($P < 0.001$), respectively. Conversely, negative correlation coefficients result from the relationships between Mg and C_{tot} contents and the elements characterizing noncarbonate terrigenous phases (Mg vs Al: −0.89; vs Fe: −0.88; vs Li: −0.89; C_{tot} vs Al: −0.95; vs Fe: −0.94; vs Li: −0.95) (Fig. 4).

H is a good index of hydrated aluminosilicates, as indicated by the excellent correlations with the elements Al, Fe, Li, Cr, Cu, and Zn.

Apart from anomalous contents in 5 samples (Fig. 4), C_{org} presents a good affinity with most of the elements determined, suggesting their partial complexing with organic matter (de Groot and others 1976). This is also remarked by the good correspondence between N and Cu and Zn and Cr (Tab. 2), since organic N comprises about 80% of the total N in the gulf sediments (Faganeli and

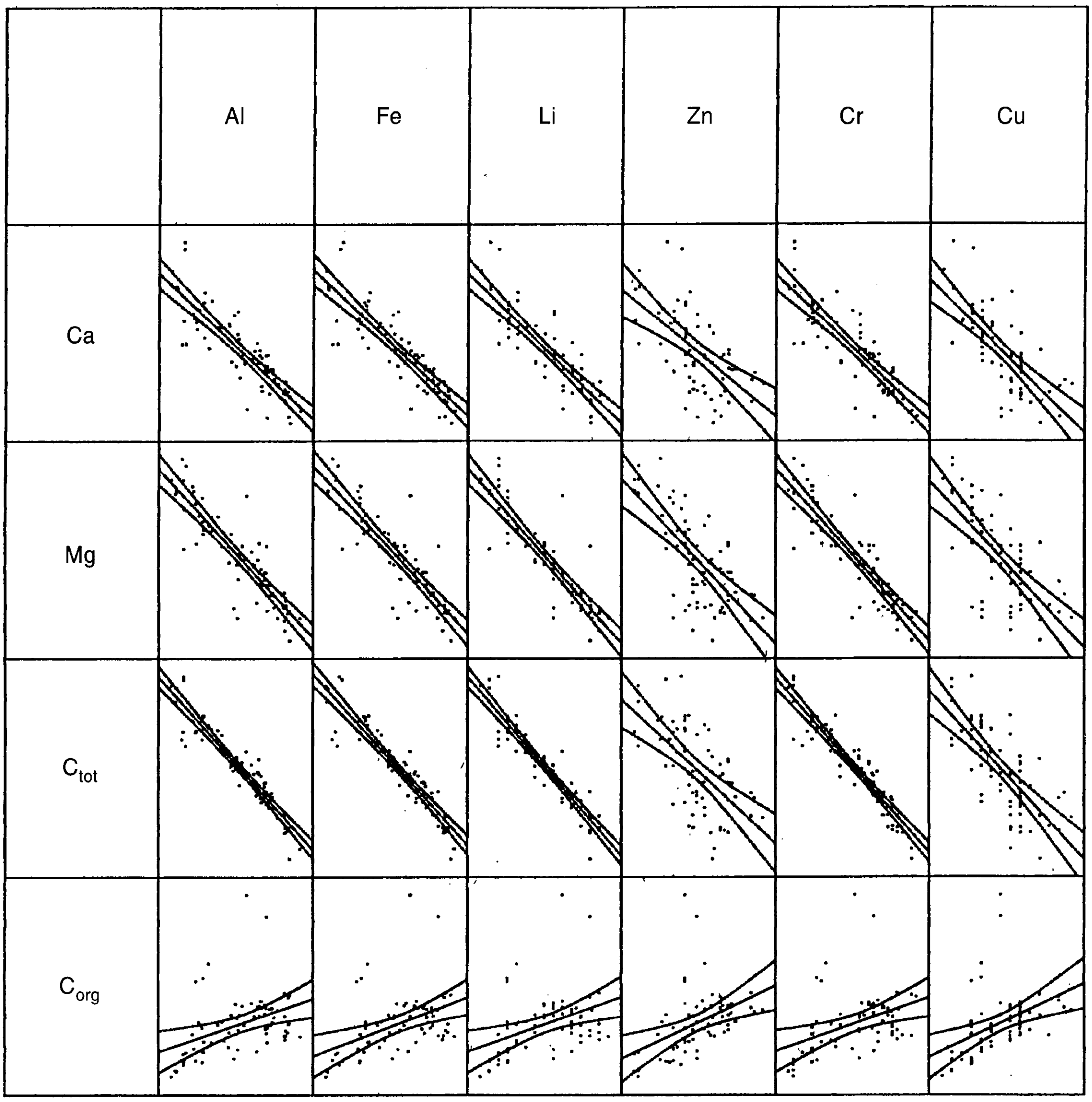

Fig. 4 Scatterplot matrix between Ca, Mg, C_{tot}, C_{org}, and Al, Fe, Li, Zn, Cr, Cu. See Fig. 2 for explanation about confidence band determination

others 1991). The anomalously high concentrations of C_{org} in the lower levels of core ISO 2 (lower reaches of Isonzo) and the whole of core IS (innermost delta) reflect local preservation of organic matter in the rapidly depositing fine sediments (Stefanini 1968).

P_{tot} shows a strong relationship with the clay fraction and thus with the Isonzo sediment supplies. A set of samples lies off the general trend due to the lower P_{tot} content (Fig. 2). They belong to cores ISO 19 and ISO 45 and to the lower part of cores ISO 39 (<40 cm depth) and ISO 40 (<20 cm depth). Their areal and vertical locations show the recent extension of Isonzo sediment over earlier deposits and the present limits of its influence, which reduces gradually seaward to the point of disappearance in the mid-gulf, where the residual sediments (mentioned earlier) outcrop.

From the correlation matrix and graphical synthesis of Fig. 2, it is evident that Al, Fe, Li, and H are the best proxies for sediment grain-size (clay) variability. As far as these elements are concerned, anthropogenic influences seem minimal, either because of their narrow 95% confidence band on plots against clay content, or because deeper levels of cores show little difference to the surficial ones, which theoretically are more exposed to recent contamination.

Because of the strong significance of the regression lines between Al and Cr and Cu and Zn, these relationships may be used to demonstrate geochemical variability in the Gulf of Trieste. Ni and Pb scatterplots denote wider dispersion. Considering Ni data, this is due to anomalously higher metal content in sandy samples from the cores collected in the river banks. Although Ni and Pb trends equally identify regionally significant functions, we recommend a careful use of the relative linear relationships for the interpretation of anomalies in the studied area.

In Fig. 5a the Zn–Al scatterplot for the Gulf of Trieste is shown with its 95% confidence band, drawn on the basis

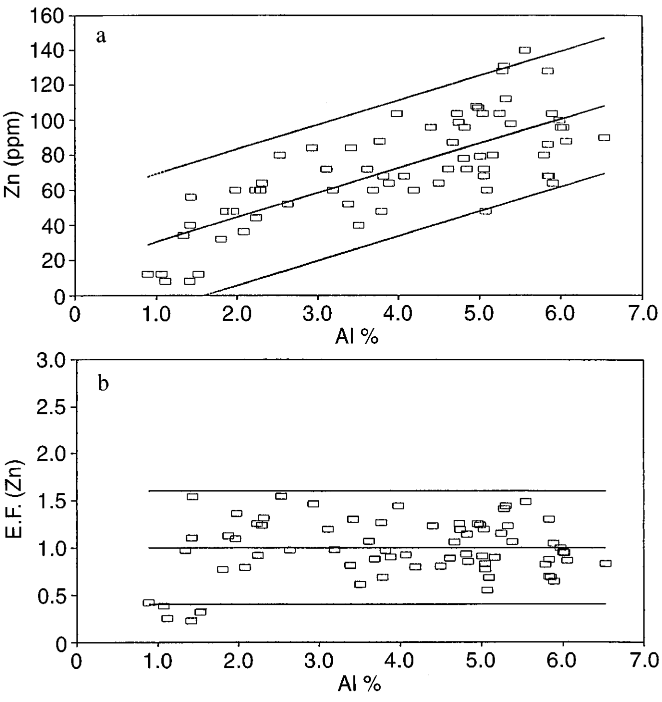

Fig. 5a, b
Bivariate relationship between: **a** Al and Zn, with the 95% confidence interval referred only to the intercept error; **b** Al and Zn (*EF*), with the 2σ range

of the standard error of *Y* determination. The same relationship is reported in terms of *EF* (Fig. 5b), i.e., the ratio between real and predicted values derived from linear normalizing functions of Tab. 3. The midline ($EF=1$) represents the coincidence between real and predicted contents of Zn, while the upper and lower lines define the $\pm 2\sigma$ range. Potentially anomalous *EF*s lie outside these lines. The *EF* may be seen as an index of contamination for a sediment sample, with respect to regional values. An $EF=3$ means that the element is 3 times higher than the calculated baseline for the study area.

The same procedure adopted in the case study of the Barcola-Bovedo disposal site (Colizza and others 1996) has led to the recognition of Zn anomalies in the sediments up to six times higher than the Gulf baseline. In order to verify the viability of the procedure, and conversely of the Barcola-Bovedo results, we compared the Zn enrichment factors determined from the baseline regression function of Isonzo cores data to *EF*s calculated by using either classical baselines or uncontaminated sediments from the neighboring areas as reference. At the same time, the almost uniform texture of the sediments (silty clays) minimized the errors due to the compulsory choice of a unique reference background value, as required by classical *EF*s.

We used Zn/Al ratios determined either from the baseline regression function of Isonzo cores data, from crustal abundance data (Taylor 1964), or from average crustal shale values (Turekian and Wedepohl 1961). We also considered for the mentioned ratio other two baselines: a fine-grained sample (about 98% mud) collected in the mid-Adriatic Sea (Paul and Meischner 1976) and a 1.3-m-deep subsurface layer, dated at 1760 AD according to ^{210}Pb analyses, from borehole MK-6 drilled to a depth of about 40 m in the Koper Bay (Faganeli and others 1991). Normalization by means of the two local backgrounds was computed using Fe as grain proxy, since Al values were not available. This procedure, in fact, can be justified by the very good correlation between Al and Fe ($r=0.990$). It should be noted, moreover, that trace metal contents were determined by Faganeli and others (1991) by using HNO_3 dissolution, which extracts, respectively, 76% of total Fe and 79% of total Zn (Donazzolo and others 1981). These two percentages are so similar that we can consider their ratio as equal to that which would have been obtained from total metal data.

Zn *EF*s calculated by means of the different baselines are compared in Fig. 6 to metal enrichment referred to the linear correlation with Al, as estimated from the Isonzo sediments. Among the different linear trends, the one that represents the dated subsurface layer of Koper Bay (not far from Trieste) as natural background provides the best correspondence with the values assessed by the related regional function. Results obtained by using average crustal shale values and abundances as reference concentrations seem to be overestimated, and this could lead to an erroneous evaluation of the effective anthropogenic influence. This fact is due to the mineralogical peculiarity of the study area, which is strongly affected by detrital carbonate supplies that dilute all the other terrigenous phases. The determination of *EF* with data provided by Paul and Meischner (1976) also underestimates the Zn enrichment, probably due to higher Zn values in the mid-Adriatic mud. Therefore, whatever the mineralogy, when the sediments are texturally homogeneous, the use of *EF*s based on either standard backgrounds or regional functions allows interpretation of the data in terms of enrichment gradient. Yet, the degree of contamination

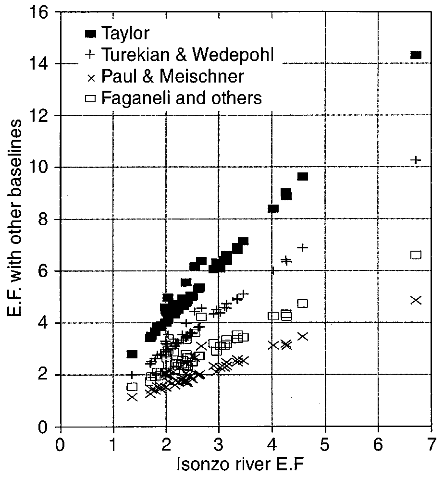

Fig. 6
Comparison among Zn EFs calculated by means of different baselines. See text for explanation

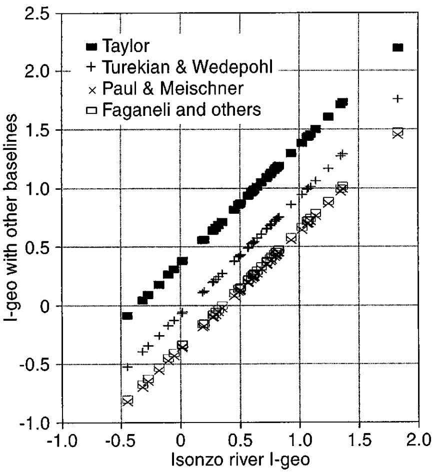

Fig. 7
Comparison among Zn Muller's I-geo calculated by means of different baselines. See text for explanation

could be obtained only with the right choice of reference baseline. In the case of textural dishomogeneity, the only choice is to use regional background functions.

We also tested the Muller's I_{geo} using Zn either from the already mentioned data or from the Isonzo sample ISO 39 E, as background value (B_n). The comparison among the results (Fig. 7) shows that the use of different baselines has little influence in the classification according to I_{geo} classes. Therefore, the procedure appears to be less sensitive in the determination of polluted samples in the Barcola-Bovedo area.

Conclusions

Earlier methods of normalizing geochemical data suffer from a number of disadvantages:

1. Allen and Rae's (1986) metal index seems a good normalization procedure but it does not quantify the degree of contamination since it does not consider a baseline.
2. Classical *EF* needs a baseline texturally and mineralogically equivalent to the sample set to be analyzed because it is sensitive to the choice of reference concentrations.
3. Muller's (1969) I_{geo} may be a quantitative measure of heavy metal contamination in sediments, but it does not take into account grain-size and natural geochemical variability owing to the use of a single reference baseline, and it tends to minimize the degree of contamination because of the numerical factor (1.5) artificially introduced.

The use of a grain-size proxy element and calculation of enrichment factors as described here permits the comparison of concentrations over a wide grain-size range and provides a simple measure of contamination based on calculated background values for texturally equivalent sediments. It also overcomes the limitations of standard backgrounds such as average shale values, which take no account of different lithological settings.

Normalization carried out using simple linear regression allows the definition of enrichment factors, which not only may define the dispersion pattern of pollutants in the marine environment but also may quantify the possible anomalies. On the basis of the sedimentological and geochemical data set of the Gulf of Trieste prepared during this study, some regional functions and consequent EF baselines have been defined, which could be useful in present and future studies of environmental quality and marine area monitoring.

Acknowledgments We wish to thank Roberto Mosca for his constant and patient supervision during the AAS geochemical analyses. Romana Melis is fully acknowledged for her help in the CHN determination. A special thanks to John Ridgway and Jadran Faganeli for the helpful suggestions and critical review of the manuscript. This research was carried out with financial support of MURST 60% funds (resp. F. Vaia)

References

Ackermann F (1980) A procedure for correcting the grain size effect in heavy metal analyses of estuarine and coastal sediments. Environ Technol Lett 1:518–527

Allen JRL and Rae JE (1987) Late Flandrian shoreline oscillations in the Severn estuary: A geomorphological and stratigraphical reconnaissance. Phil Trans R Soc London B315:185–230

Brambati A (1968) Mixing and settling of fine terrigenous material (<16 μm) in the northern Adriatic Sea between Venice and Trieste. St Trent Sc Nat A45:103–117

Brambati A (1970) Provenienza, trasporto e accumulo dei sedimenti recenti nelle lagune di Marano e di Grado e nei litorali tra i fiumi Isonzo e Tagliamento. Mem Soc Geol It 9:281–329

Brambati A and Catani G (1988) Le coste e i fondali del Golfo di Trieste dall'Isonzo a Punta Sottile: Aspetti geologici, geomorfologici, sedimentologici e geotecnici. Hydrores Trieste 6:13–28

Brambati A and Marocco R (1984) Le discariche dei residui di lavorazione di bauxiti, fluorine e fosforiti nel Golfo di Venezia. Ist Ven Sc Lett Ed Arti (Rapp Studi) 9:369–402

Brambati A and Venzo GA (1967) Recent sedimentation in the northern Adriatic Sea between Venice and Trieste. St Trent Sc Nat A44:202–274

Brambati A, Catani G, and Marocco R (1982) Il litorale sabbioso del Friuli-Venezia Giulia: trasporto, dispersione e deposizione dei sedimenti della spiaggia sottomarina. Boll Soc Adriatica Sci 65:1–32

Brambati A, Ciabatti M, Fanzutti GP, Marabini F, and Marocco R (1983) A new sedimentological textural map of the northern and central Adriatic Sea. Boll Oceanol Teor Appl 1:267–271

Bruland KW, Bertine K, Koide M, and Goldberg ED (1974) History of metal pollution in southern California coastal zone. Environ Sci Technol 8:425–432

Ciavola P and Covelli S (1994) Coastal-estuary flux of heavy metals: The use of estuarine salt marshes as a recorder of pollution in the Humber Estuary, UK. Proceedings, II International Symposium, Littoral '94 Eurocoast, Lisbon, 26–29 Sept 1994. 1:231–245

Colizza E, Fontolan G, and Brambati A (1996) Impact of a coastal disposal site for inert wastes on the physical marine environment, Barcola-Bovedo, Trieste, Italy. Environ Geol 27:270–285

de Groot AJ, Salomons W, and Allersma E (1976) Processes affecting heavy metals in estuarine sediments. In: Burton JD and Liss PS (Eds), Estuarine chemistry. London: Academic Press. pp 131–157

De Rosa S, Damiani V, and Ambrosano E (1981) Indagine sullo stato di contaminazione dei sedimenti superficiali del tratto del Golfo di Napoli tra Capo Posillipo e Torre del Greco. Atti Convegno Unità Afferenti ai Sottoprogetti Risorse Biol e Inquin Marino. pp 625–642

Din TB (1992) Use of aluminium to normalize heavy-metal data from estuarine and coastal sediments of Straits of Melaka. Mar Pollut Bull 24:484–491

Donazzolo R, Hieke Merlin O, Menegazzo Vitturi L, Orio AA, Pavoni B, Perin G, and Rabitti S (1981) Heavy metal contamination in surface sediments from the Gulf of Venice, Italy. Mar Pollut Bull 12:417–425

Faganeli J, Planinic R, Pedzic J, Smodis B, Stegnar P, and Ogorelec B (1991) Marine geology of the Gulf of Trieste (northern Adriatic): Geochemical aspects. Mar Geol 99:93–108

Ferguson JE (1990) The heavy elements: Chemistry, environmental impact and health effects. New York: Pergamon Press, 412 pp

Gaudette HE, Flight WR, Toner L, and Folger DW (1974) An inexpensive filtration method for the determination of organic carbon in recent sediments. J Sediment Petrol 44:249–253

Giorgetti F, Mosetti F, and Macchi G (1968) Caratteristiche morfologiche, fisiche e chimiche del fondo marino del Golfo di Trieste nell'area compresa entro la congiungente Punta Grossa-Bocche di Primero. Boll Soc Adr Sc 1:3–21

Grant A and Middleton R (1990) An assessment of metal contamination of sediments in the Humber Estuary, UK. Estuar Coast Shelf Sci 31:71–85

Guerzoni S, Frignani M, Giordani P, and Frascari F (1984) Heavy metals in sediments from different environments of a northern Adriatic Sea area, Italy. Environ Geol Water Sci 6:111–119

Helz GR, Sinex SA, Setlock GH, and Cantillo AY (1983) Chesepeake Bay study trace elements. EPA-600/3-83-012. Annapolis, MD: US Environmental Protection Agency

Hirst DM (1962) The geochemistry of modern sediments from the Gulf of Paria – II. Geochim Cosmochim Acta 26:1147–1187

Loring DH (1978) Geochemistry of zinc, copper, and lead in the sediments of the estuary and Gulf of St Lawrence. Can J Earth Sci 15:757–772

Loring DH (1990) Lithium – a new approach for the granulometric normalization of trace metal data. Mar Chem 29:155–168

Loring DH and Nota DJG (1973) Morphology and sediments of the Gulf of St Lawrence. Fish Res Board Can Bull 182:147 pp

Loring DH and Rantala RTT (1992) Manual for the geochemical analyses of marine sediments and suspended particulate matter. Earth Sci Rev 32:235–283

Majori L, Nedoclan G, and Modonutti GB (1976) Inquinamento da mercurio nell'Alto Adriatico. Acqua Aria 3:164–172

Macchi G (1968) Sulla composizione chimica dei sediment recenti nel Golfo di Trieste. Boll Soc Adriat Sci 56:22–41

Middleton R and Grant A (1990) Heavy metals in the Humber estuary: *Scrobicularia* clay as a preindustrial datum. Proc Yorkshire Geol Soc 48:75–80

Muller G (1969) Index of geoaccumulation in sediments of the Rhine River. Geojournal 2:108–118

Nota DJG (1958) Sediments of the western Guiana shelf. Reports of the Orinoco Shelf Expedition Vol II. Meded Landbouwhogesch Wageningen 58:1–98

Ogorelec B, Misic M, and Faganeli J (1991) Marine geology of the Gulf of Trieste (northern Adriatic): Sedimentological aspects. Mar Geol 99:79–91

Paul J and Meischner D (1976) Heavy metal analyses from sediments of the Adriatic Sea. Senckemb Maritt 8:91–102

Pavoni B, Donazzolo R, Marcomini A, De Gobbi D, and Orio AA (1987) Historical development of the Venice Lagoon contamination as recorded in radiodated sediment cores. Mar Pollut Bull 18:18–24

Prohic E and Juracic M (1989) Heavy metals in sediments – problems concerning determination of the anthropogenic influence. Study in the Krka river estuary, eastern Adriatic coast, Yugoslavia. Environ Geol Water Sci 13:145–151

Rand MC, Greenberg AE, and Taras MJ (1976) Standard methods for the examination of water and wastewater. XIV Ed WPCF APHA AWWA. 1193 pp

Rule JP (1986) Assessment of trace element geochemistry of Hampton Roads Harbor and lower Cheseapeake Bay area sediments. Environ Geol Water Sci 8:209–219

Selli R, Frignani M, and Giordani P (1977) Aspetti scientifici dell'inquinamento dei mari italiani. Accad Naz Lincei Rome Atti Convegni 31:169–191

Siegel FR, Slaboda ML, and Stanley DJ (1994) Metal pollution loading, Manzalah Lagoon, Nile Delta, Egypt: Implications for aquaculture. Environ Geol 23:89–98

Sinex SA and Helz GR (1981) Regional geochemistry of trace elements in Chesapeake Bay sediments. Environ Geol 3:315–323

Sinex SA and Wright DA (1988) Distribution of trace metals in the sediments and biota of Chesapeake Bay. Mar Pollut Bull 19:425–431

Stefanini S (1968) Distribuzione dei carbonati di Ca e Mg nelle sabbie dei fiumi tributari dell'Adriatico settentrionale tra Venezia e Trieste e dei loro principali affluenti. Studi Trent Sc Nat A45:101–124

Stefanini S (1970–71) Distribuzione del Li, Na, K, Sr, Cr, Mn, Fe, Ni, Cu, Zn e Pb nei sedimenti superficiali dell'Adriatico Settentrionale fra Venezia e Trieste. Mem Mus Trid Sc Nat 18:173–213

Stefanini S (1976) Composizione delle acque fluviali del Friuli-Venezia Giulia durante la fase di magra e di piena dei corsi d'acqua. CNR Quad Ist Ric Acque 28:391–447

Taylor SR (1964) The abundance of chemical elements in the continental crust – a new table. Geochim Cosmochim Acta 28:1273–1285

Trefry JH and Presley BJ (1976) Heavy metals in sediments from San Antonio Bay and the northwest Gulf of Mexico. Environ Geol 1:282–294

Turekian KK and Wedepohl KH (1961) Distribution of the elements in some major units of the earth's crust. Bull Geol Soc Am 72:175–191

Van Straaten LMJU (1965) Sedimentation in the north-western part of the Adriatic Sea. A symposium. Colston Res Soc 17:142–162

Windom HL, Schropp SJ, Calder FD, Ryan DJ, Smith RG Jr, Burney LC, Lewis FG, and Rawlinson CH (1989) Natural trace metal concentrations in estuarine and coastal marine sediments of the southeastern United States. Environ Sci Technol 23:314–320